Published in final edited form as:
J Hepatol. 2010 May ; 52(5): 718–726. doi:10.1016/j.jhep.2009.12.027.

Postnatal paucity of regulatory T cells and control of NK cell activation in experimental biliary atresia

Alexander G. Miethke[*], **Vijay Saxena**, **Pranavkumar Shivakumar**, **Gregg E. Sabla**, **Julia Simmons**, and **Claire A. Chougnet**
Division of Pediatric Gastroenterology, Hepatology and Nutrition, Cincinnati Children's Hospital Medical Center, MLC 2010, 3333 Burnet Avenue, Cincinnati, OH 45229-3039, USA

Department of Pediatrics, University of Cincinnati, College of Medicine, Cincinnati, OH, USA

Division of Pediatric Gastroenterology, Hepatology and Nutrition, Cincinnati Children's Hospital Medical Center, 3333 Burnet Avenue, Cincinnati, OH 45229-3039, USA

Abstract

Background & Aims—Although recent studies have identified important roles for T and NK cells in the pathogenesis of biliary atresia (BA), the mechanisms by which susceptibility to bile duct injury is restricted to the neonatal period are unknown.

Methods—We characterised hepatic regulatory T cells (Tregs) by flow cytometry in two groups of neonatal mice challenged with rhesus rotavirus (RRV) at day 7 (no ductal injury) or day 1 of life (resulting in BA), determined the functional interaction with effector cells in co-culture assays, and examined the effect of adoptive transfer of CD4+ cells on the BA phenotype.

Results—While day 7 RRV infection increased hepatic Tregs (Foxp3+ CD4+ CD25+) by 10-fold within 3 days, no increase in Tregs occurred at this time point following infection on day 1. *In vitro*, Tregs effectively suppressed NK cell activation by hepatic dendritic cells and decreased the production of pro-inflammatory cytokines, including TNFα and IL-15, following RRV infection. *In vivo*, adoptive transfer of CD4+ cells prior to RRV inoculation led to increased survival, improved weight gain, decreased population of hepatic NK cells, and persistence of donor Tregs in the liver.

Conclusions—1) The liver is devoid of Tregs early after perinatal RRV infection; 2) Tregs suppress DC-dependent activation of naive NK cells *in vitro*, and Treg-containing CD4+ cells inhibit hepatic NK cell expansion *in vivo*. Thus, the postnatal absence of Tregs may be a key factor that allows hepatic DCs to act unopposed in NK cell activation during the initiation of neonatal bile duct injury.

Keywords

Regulatory T cells; Experimental biliary atresia; NK cell activation; Neonatal biliary injury

*Corresponding author: Alexander G. Miethke, Cincinnati Children's Hospital Medical Center, Division of Pediatric, Gastroenterology, Hepatology and Nutrition, MLC 2010, 3333 Burnet Avenue, Cincinnati, OH 45229-3039, USA, Tel.: +1 513 636 9078; fax: +1 513 636 5581, alexander.miethke@cchmc.org (A.G. Miethke).

Financial disclosure: none

The authors who have taken part in this study declared that they do not have anything to declare regarding funding from industry or conflict of interest with respect to this manuscript.

Introduction

Biliary atresia (BA) is a progressive necroinflammatory obstruction of the extrahepatic biliary tree that leads to chronic cholestasis and end-stage liver disease in children. Although the aetiology and pathogenesis of BA are largely unknown, the coordinated activation of pro-inflammatory genes with prominent expression of interferon-γ [1] and oligoclonal expansion of T cells in liver tissue obtained at the time of diagnosis [2] suggest that BA is an immune-mediated disease.

Because initiation of bile duct injuries cannot be studied directly in humans, investigators have used a well-established mouse model of BA to pursue mechanistic experiments [3]. In this model, intraperitoneal injection of Rhesus Rotavirus (RRV) into BALB/c mice within the first 3 days of life causes inflammatory biliary obstruction by 7 days and onset of jaundice, closely recapitulating the human disease. Inactivation of interferon-γ and targeted depletion of lymphocyte subpopulations have revealed key roles for interferon-γ, CD8+ and natural killer (NK) cells for the initiation of neonatal bile duct obstruction [4–6].

Whether immaturity of the developing immune system is linked to the initiation of bile duct injury and restriction of BA to the perinatal period is currently unknown. In mice, neonatal immaturity of the adaptive immune system is particularly striking with regard to regulatory T cells (Tregs). Natural Tregs, which represent a small percentage of the CD4+ T cells that are indispensable for the maintenance of peripheral tolerance and prevention of autoimmune disease [7], are not generated in the thymus before 3 days of age [8]. Therefore, we hypothesised that the susceptibility of neonatal mice to experimental BA was linked to an immature Treg response to perinatal viral challenge. Here, we found evidence that Tregs were absent during early immune responses in experimental BA, whereas their prompt emergence in the liver following viral challenge was associated with prevention of disease in older mice. In mechanistic experiments, Tregs were shown to inhibit hepatic NK cell activation by neonatal dendritic cells following RRV infection *in vitro*. Importantly, adoptive transfer of CD4+ cells attenuated the BA phenotype *in vivo*.

Material and methods

Human subjects

Liver samples for gene expression analysis were taken by wedge biopsy from 2–3-month-old infants undergoing intraoperative cholangiograms and Kasai portoenterostomies at the time of diagnosis of BA at Children's Hospital Medical Center in Cincinnati, OH. The diagnosis was confirmed by histology of the portal plate, which demonstrated bile duct obstruction.

Samples from children without liver disease were obtained from liver donors at 2–3.5 years of age at the University of Chicago and served as controls. Liver samples from precisely age-matched healthy controls could not be obtained due to ethical concerns. The studies were approved by the institutional review boards of both institutions, and informed consent was obtained from the infants' legal guardians.

Gene expression in human liver samples

Total RNA was isolated from frozen liver tissue using an RNeasy kit (Qiagen, Valencia, Spain) according to the manufacturer's instructions and subjected to quantitative real-time PCR on a Stratagene Mx-4000 Multiplex Quantitative PCR sequence detector (Stratagene, La Jolla) as described previously [6], using specific primers (Supplemental Table 1) and *HPRT* as a housekeeping gene.

Mouse Model of BA

A total of 1.5×10^6 focus-forming units (ffu) of RRV were injected intraperitoneally (i.p.) into BALB/c pups within the first 24 hours of life (group A), as described previously [3,6,9]. For group B, a dose of 1×10^6 ffu of RRV/gram body weight was administered i.p. on day 7 of life. All protocols were approved by the Institutional Animal Care and Use Committee.

Mononuclear cell (MNC) isolation and flow cytometric analysis

MNCs were isolated from livers and spleens by gentle mincing and passage through a 40-μm cell strainer, centrifuged and resuspended in 33% Percoll (Sigma, St. Louis), followed by centrifugation at 400*g* at RT for 20 min and red cell lysis. Phenotyping was performed as described previously [4], using the following antibodies: FITC-CD4, PE-CD8, APC-CD49b (NK), biotin-CD103 (all BD Biosciences, San Jose), and PE-CD25 (Miltenyi Biotec, Auburn). Intracellular staining with APC-Foxp3 or biotin-CTLA-4 (both from eBioscience, San Diego) was performed following surface staining and treatment with fixation/permeabilisation buffer (eBioscience) according to the manufacturer's instructions. Biotin-conjugated antibody staining was followed by staining with APC-streptavidin (eBioscience). Stained cells were analysed with a FACSCalibur (BD Bioscience). Data were analysed with CellQuest (BD Biosciences) or FlowJo (Tree Star, Inc., Stanford).

Gene expression in purified Tregs

Tregs were purified from pooled livers or spleens by magnetic-bead-based separation according to the manufacturer's instructions (Treg cell isolation kit, Miltenyi Biotec). With regard to purity, CD4+ CD25+ cells made up was 93% of live cells, as determined by FACS analysis. Total RNA was purified (microRNeasy, Qiagen), and target mRNA concentrations were quantified by real-time RT-PCR as described above.

Treg suppression assay

CD4+ cells were enriched from splenic cell suspensions using CD4 Microbeads (Miltenyi Biotec) prior to sorting CD4+ CD25+ Treg and CD4+ CD25− responder T(resp) cells on a FACSVantage (Becton Dickinson). Irradiated splenocytes from neonatal RRV-infected mice were used as APC. A total of 30,000 Tresp cells were co-cultured with graded ratios of Tregs and 100,000 APC in 200 μl complete RPMI-10 in 96-well U–bottom plates coated with anti-CD3 (1 μg/ml, eBioscience) for 72 hours. The compound ^{3}H-thymidine (1 μl/well) was added for the last 16 hours of culture, and levels of incorporated radioactivity were determined using a TopCount NXT scintillation counter.

Treg inhibition of NK cytotoxicity to cholangiocytes

Hepatic NK cells and splenic Tregs were purified using CD49b (DX5) Microbeads and the Treg isolation kit (both Miltenyi Biotec), respectively. NK cell-induced lysis of cholangiocytes was measured in a chromium release assay, as described previously [4].

Treg inhibition of dendritic-cell dependent NK activation

For hepatic dendritic cell (DC) isolation, livers were gently minced and digested with Collagenase-D (1 mg/ml, Roche Diagnostics, Indianapolis, IN) for 30 min at 37°C prior to passage through a 40-μm cell strainer, Percoll gradient centrifugation and positive selection of CD11c+ and PDCA-1+ DCs (Pan-DC isolation kit, Miltenyi Biotec). Hepatic NK cells and splenic Tregs were purified as described above. A total of 50,000 NK cells/well alone, in co-culture with DCs (1:1) or with DCs and Tregs (1:1:1) were cultured in triplicate in complete RPMI-10 for 24 hours prior to staining with FITC-CD49b (BD Bioscience) and PE-CD69 or PE-NKG2D/CD314 (both from eBioscience). Aliquots were removed from supernatants after

24 hours of culture for multiplex cytokine determination using the LINCOplex® Multiplex Immunoassay kit (Millipore, St. Charles) according to the manufacturer's protocols. Concentrations were calculated from standard curves using recombinant proteins.

Adoptive transfer of CD4+ cells

Splenic CD4+ cells were purified from adult BALB/c mice using Pan-T-cell columns (R&D systems, Minneapolis) and positive CD4+ separation with subsequent bead removal (FlowComp CD4+ Dynabeads, Invitrogen, Carlsbad) according to the manufacturers' protocols. FACS analysis confirmed that 95% of live cells were CD4+, and approximately 10% of these cells stained positive for CD25. Cells (10×10^6) suspended in PBS were injected i.p. into neonatal pups on day 2 of life, followed by RRV injection one day later. Age-matched controls were subjected to the same protocol, with the exception that the pups were administered saline on day 2 followed by RRV inoculation on day 3. Donor mice were of Thy1.2 BALB/c background, while the lymphocytes of recipient mice expressed Thy1.1, facilitating tracking of donor cells after adoptive transfer. Thy1.1 BALB/c mice were a generous gift from Dr. Suzanne Morris (Division of Immunobiology at Cincinnati Children's Hospital Medical Center).

Statistical analysis

Values are expressed as mean ±standard deviation (S.D.), and statistical significance was determined by an unpaired t-test with a significance set at $p<0.05$. Kaplan and Meier survival curves were created using Graph Pad Prism (Graph Pad Software, LaJolla). The numbers of animals (N) studied per experiment are presented in the figure legends.

Results

Treg signature genes are upregulated in livers of infants with BA

mRNA for genes encoding suppressor cytokines (*IL-10, TGFβ1*) and genes associated with T cell commitment to a regulatory phenotype (*CD4, CTLA4, FOXP3)* were significantly increased in livers from nine infants with BA at the time of diagnosis compared to seven paediatric controls without liver disease (Fig. 1). To define the role of Tregs during initiation of neonatal ductal injury, we studied the kinetics of the emergence of Tregs in liver and lymphoid tissues in the murine model of BA.

Liver and secondary lymphoid tissues are devoid of Tregs during the immediate postnatal period

Hepatic and splenic MNCs from non-infected 3- and 7-day-old neonatal and adult mice were analysed by flow cytometry, revealing a reduced frequency of CD4+ lymphocytes in the livers and spleens of 3-day-old mice compared to 7-day-old mice. Tregs, defined by the expression of the Treg surface markers CD4 and CD25 and the transcription factor Foxp3 [10], were almost completely absent in both organs at 3 days of life. Thereafter, between 3 and 7 days of life, the percentage of CD4+ lymphocytes co-expressing Foxp3+ and CD25+ increased by 3- and 6-fold in the liver and spleen, respectively (Fig. 2A–B); at 7 days, the frequency of hepatic and splenic Tregs was only slightly reduced compared to the levels observed in adult mice.

Infection with RRV at birth fails to induce prompt Treg response in liver or lymphoid tissue

Inoculation of RRV within 24 hours of life (group A) led to BA manifesting as jaundice, acholic stool, and bilirubinuria by 7 days and death by 15 days of life in 100% of RRV-infected pups, as described previously [6]. The Treg frequency and phenotype were investigated at two time points following RRV challenge: before the onset of cholestasis (3 days after infection) and during the symptomatic phase (at 7 days; experimental design Fig. 3A). The numbers of CD4

+ CD25+ Foxp3+ lymphocytes in the liver and spleen were quantified by flow cytometry. In addition, expression of CTLA4, which is associated with Treg suppressor function [11], and CD103, a marker of Treg homing to inflamed epithelium [12], was investigated. Importantly, the numbers of CD4+ CD25+ Tregs expressing Foxp3, CD103 or CTLA4 remained low in both the liver (Fig. 3C) and the spleen (Fig. 3E) 3 days after RRV infection, at levels comparable to saline-injected age-matched controls. By 7 days after injection, the total number of Foxp3 +, CD103+ and CTLA4+Tregs per liver increased by 15-, 19- and 85-fold, respectively, compared to age-matched controls (Fig. 3C).

In contrast, mice did not develop cholestasis following RRV injection at 7 days of age (group B). Notably, the numbers of hepatic Foxp3+, CD103+ and CTLA4 + Tregs increased by 10-, 11- and 6-fold, respectively, compared to age-matched saline controls during the early response to RRV challenge (day 3 after infection, Fig. 3D). The increase in Tregs in lymphatic tissue (spleen) corresponded with hepatic Treg expansion in both groups (Fig. 3E–F).

Neonatal Tregs display an activated phenotype following RRV infection

To determine the functional profile of neonatal Tregs emerging after RRV infection, mRNA expression levels of candidate genes of Treg activation [13,14] were determined in freshly purified hepatic and splenic Tregs. In group A, hepatic and splenic Tregs express similar genes in infected or saline control mice 3 days after injection (data not shown). However, *IL-10*, *Granzyme A* and *Perforin* expression were increased above control levels by >10 fold in hepatic Tregs 7 days after viral challenge (Fig. 4A). In Group B, mRNA expression of *Granzyme A*, *GITR* and *IL-10* were upregulated in splenic Tregs from infected mice by >2 fold over controls by 3 days after inoculation (Fig. 4D).

Neonatal Tregs exert suppressor function

To directly determine the suppressor function of neonatal Tregs, we co-cultured CD4+ CD25 + Tregs with autologous CD4+ CD25− responder cells from RRV-infected neonatal mice in conventional proliferation assays. Because of the low numbers of Tregs populating the neonatal liver and the similar Treg responses in the liver and spleen following RRV infection, these assays were only performed with splenic Tregs. Proliferation was significantly suppressed in co-cultures at Treg:Tresp ratios of 1:1 and 1:2 for group A (Fig. 4E) and for ratios of 1:1 to 1:4 in group B (Fig. 4F).

Tregs suppress DC-dependent activation of hepatic NK cells and production of pro-inflammatory cytokines

Because hepatic NK cells are key effector cells of bile duct injury in experimental BA [5], we tested whether Tregs are able to directly inhibit NK function. Hepatic NK cells from RRV-infected neonatal mice killed cholangiocytes *in vitro* within 5 hours of contact in a dose-dependent fashion (Fig. 5A). The addition of Tregs at a 1:1 ratio with NK cells did not significantly alter NK-mediated killing of cholangiocytes, producing a similar killing profile for respective target: effector ratios ($p = 0.4$).

To determine the effect of Tregs on DC-mediated activation of hepatic NK cells in neonatal mice, we designed a co-culture assay based on *in vitro* studies established in other experimental systems [15,16]. *In vivo* primed DCs from livers of mice infected at birth were purified 3 days after inoculation and co-cultured with NK cells from livers of non-infected, age-matched mice. Increased expression of the activation marker CD69 and, to a lesser extent, NKG2D, on NK cells, as quantified by mean fluorescence intensity (MFI) and frequency of CD69+ (NKG2D +) NK cells, was observed in co-cultures of NK cells with DCs from RRV-infected mice compared to control assays using DCs from saline-injected animals. Importantly, DC-dependent activation of NK cells was inhibited when Tregs were added to the co-culture (Fig

5B). Furthermore, production of pro-inflammatory cytokines (TNFα, IL-15, IL12p70, IL-17, IFNγ and IL-6) was reduced by varying degrees in the presence of Tregs (Fig 5C). Control experiments included cultures of RRV-primed hepatic DCs cultured alone, in which cytokine production [mean in pg/ml] was minimal for IFNγ [38] and IL-6 [78] or below the detection limit for IL15, IL12p70 and IL17. Minimal production of IFNγ [47] and IL6 [19] was found in cultures of unstimulated NK cells without DCs present or in co-culture with DCs from non-infected neonatal mice, which also produced only low levels of IFNγ [8] and IL-6 [93] (data for control experiments not shown).

Adoptive transfer of CD4+ cells attenuates the BA phenotype

The adoptive transfer of 10×10^6 splenic CD4+ cells, estimated to contain approximately 1×10^6 Tregs, doubled the median survival time from 10 to 20 days (Fig. 6A), and weight gain improved substantially compared to age-matched, RRV-infected controls (Fig 6B). Furthermore, adoptive transfer caused a 3-fold decrease in hepatic NK cells during the pre-symptomatic period (Day 5 post-RRV, Fig. 6C) and a reduction in hepatic CD4+ and CD8+ cells by 3- and 2-fold, respectively, during the later stage of biliary injury (Day 13 post-RRV, Fig. 6D). Of note, this reduction was accompanied by a 2.4-fold increase in hepatic Tregs, 63% of which were of donor (Thy1.2+) origin (Fig. 6D). Collectively, our data suggest that CD4+ cells, specifically regulatory CD4+ cells, play important roles in the control of NK-cell expansion and activation in experimental BA.

Discussion

We found that the postnatal absence of Tregs from liver and lymphoid tissues during ontogeny critically affects the immune response to perinatal RRV infection in experimental BA, as Tregs were absent during the early immune response in mice injected with RRV on day 1 but emerged quickly in the liver and spleen after virus inoculation on day 7. Based on functional studies showing that Tregs are able to inhibit DC-dependent activation of NK cells in the neonatal liver, we linked the numeric paucity of Tregs during the early postnatal period to enhanced activation of chief effector cells in experimental BA. *In vivo*, the adoptive transfer of CD4+ cells led to the persistence of donor Tregs in the liver, which was associated with decreased expansion of hepatic NK cells and significant attenuation of the BA phenotype.

Postnatal delay in murine Treg development has been implicated as the cause of the development of strain-specific experimental autoimmunity [17,18]. Our studies clearly show that under physiologic and pathologic conditions related to perinatal RRV infection, liver and lymphoid tissues are devoid of Tregs during the time period of susceptibility to experimental BA. Neonatal Tregs, emerging after RRV infection on day 7, display an activated molecular phenotype and exert suppressor function, which further supports our conclusion that Tregs contribute to attenuation of the inflammatory response to viral challenge and subsequent biliary injury in older mice. Based on these data, we raise the possibility that the absence of Tregs in the first 3 days of life renders the newborn liver susceptible to an unrestrained pro-inflammatory response to a viral challenge.

The robust increase in hepatic Tregs 7 days after perinatal RRV infection at the time of inflammatory bile duct obstruction in murine BA appears to correlate with our observation of upregulation of Treg signature genes in the livers of infants with BA compared to livers from paediatric subjects without liver disease. Definition of Tregs in humans is difficult, as all markers, including FOXP3, are also transiently upregulated in activated T cells [19]. Nevertheless, concomitant increases in FOXP3, CTLA4, CD4 and IL-10 support our conclusion that Treg frequency and/or activation are increased in the livers of infants with BA at the time of diagnosis. Further prospective studies, including suppression assays and analysis

of FOXP3 epigenetic modifications with precisely age-matched controls, will be needed to validate our findings.

In mechanistic studies performed in the murine model, we linked the paucity of Tregs during the immediate post-natal period to enhanced DC-dependent activation of NK cells as effector cells of bile duct injury in experimental BA [5]. To our knowledge, this is the first study directly investigating the role of Tregs in the modulation of DC-dependent activation of innate immune cells in the neonatal liver. Furthermore, our results are consistent with reports indicating that T cells can interrupt the positive feedback loop between NK cells and APC through the inhibition of TNFα production by CD11c+ DCs, as shown in models of Poly I:C-induced innate "cytokine storm" and of neonatal liver failure [20,21]. The precise mechanisms for the interaction between Tregs and innate immune cells are still unclear. One potential mechanism is the modulation of activation of myeloid DCs [7] through the formation of aggregates around DCs and downregulation of CD80 and CD86 in a cell contact/CTLA-4-dependent manner [22].

Importantly, we showed that the adoptive transfer of CD4+ cells into neonatal mice leads to the persistence of donor Tregs in the liver, decreased expansion of hepatic NK cells following RRV infection and, subsequently, attenuation of the BA phenotype. Although these experiments did not directly examine the specific contribution of Tregs *in vivo*, they strongly support our hypothesis. In particular, they are consistent with our *in vitro* observations of Treg control of NK activation. Future experiments will be needed to identify the immunoregulatory circuits involved in the control of the innate and adaptive immune systems in RRV-induced neonatal bile duct injury.

Supplementary Material

Refer to Web version on PubMed Central for supplementary material.

Acknowledgments

A.G.M was supported by the American Liver Foundation Liver Scholar Award and is recipient of a Pilot and Feasibility Award from the Cincinnati Digestive Health Center (P30 DK078392). The work was also supported by the NIH grant R01 AI068524 (to CAC).

We thank Dr. William Balistreri (from Cincinnati Children's Hospital Medical Center) for reviewing the manuscript and providing insightful comments and Christy Caudill (Division of Rheumatology, Cincinnati Children's Hospital Medical Center) for technical assistance with the ^{3}H-Thymidine proliferation assay.

Abbreviations

BA	biliary atresia
RRV	Rhesus Rotavirus
NK	natural killer
Tregs	regulatory T cells
PCR	polymerase chain reaction
ffu	fluorescence-forming unit
i.p	intraperitoneally
MNC	mononuclear cell
APC	antigen presenting cells

FACS	fluorescence activated cell sorting
DC	dendritic cell
SD	standard deviation
MFI	mean fluorescence intensity

References

1. Bezerra JA, Tiao G, Ryckman FC, Alonso M, Sabla GE, Shneider B, et al. Genetic induction of proinflammatory immunity in children with biliary atresia. Lancet 2002;23:1653–1659. [PubMed: 12457789]
2. Mack CL, Falta MT, Sullivan AK, Karrer F, Sokol RJ, Freed BM, et al. Oligoclonal expansions of CD4+ and CD8+ T-cells in the target organ of patients with biliary atresia. Gastroenterology 2007;133:278–287. [PubMed: 17631149]
3. Riepenhoff-Talty M, Schaekel K, Clark HF, Mueller W, Uhnoo I, Rossi T, et al. Group A rotaviruses produce extrahepatic biliary obstruction in orally inoculated newborn mice. Pediatr Res 1993;33:394–399. [PubMed: 8386833]
4. Shivakumar P, Sabla G, Mohanty S, McNeal M, Ward R, Stringer K, et al. Effector role of neonatal hepatic CD8+ lymphocytes in epithelial injury and autoimmunity in experimental biliary atresia. Gastroenterology 2007;133:268–277. [PubMed: 17631148]
5. Shivakumar P, Sabla G, Whitington P, Chougnet C, Bezerra JA. Neonatal NK cells target the mouse duct epithelium via Nkg2d and drive tissue-specific injury in experimental biliary atresia. J Clin Invest 2009;119:2281–2290. [PubMed: 19662681]
6. Shivakumar P, Campbell KM, Sabla GE, Miethke A, Tiao G, McNeal MM, et al. Obstruction of extrahepatic bile ducts by lymphocytes is regulated by IFN-gamma in experimental biliary atresia. J Clin Invest 2004;114:322–329. [PubMed: 15286798]
7. Kim JM, Rasmussen JP, Rudensky AY. Regulatory T cells prevent catastrophic autoimmunity throughout the lifespan of mice. Nat Immunol 2007;8:191–197. [PubMed: 17136045]
8. Fontenot JD, Dooley JL, Farr AG, Rudensky AY. Developmental regulation of Foxp3 expression during ontogeny. J Exp Med 2005;202:901–906. [PubMed: 16203863]
9. Petersen C, Biermanns D, Kuske M, Schakel K, Meyer-Junghanel L, Mildenberger H. New aspects in a murine model for extrahepatic biliary atresia. J Pediatr Surg 1997;32:1190–1195. [PubMed: 9269968]
10. Fontenot JDGM, Rudensky AY. Foxp3 programs the development and function of CD4+CD25+ regulatory T cells. Nat Immunol 2003;4:330–336. [PubMed: 12612578]
11. Sansom DM, Walker LS. The role of CD28 and cytotoxic T-lymphocyte antigen-4 (CTLA-4) in regulatory T-cell biology. Immunol Rev 2006;212:131–148. [PubMed: 16903911]
12. Eksteen B, Miles A, Curbishley SM, Tselepis C, Grant AJ, Walker LS, et al. Epithelial inflammation is associated with CCL28 production and the recruitment of regulatory T cells expressing CCR10. J Immunol 2006;177:593–603. [PubMed: 16785557]
13. McHugh RS, Whitters MJ, Piccirillo CA, Young DA, Shevach EM, Collins M, et al. CD4(+)CD25 (+) immunoregulatory T cells: gene expression analysis reveals a functional role for the glucocorticoid-induced TNF receptor. Immunity 2002;16:311–323. [PubMed: 11869690]
14. Zelenika D, Adams E, Humm S, Graca L, Thompson S, Cobbold SP, et al. Regulatory T cells overexpress a subset of Th2 gene transcripts. J Immunol 2002;168:1069–1079. [PubMed: 11801640]
15. Dalod M, Hamilton T, Salomon R, Salazar-Mather TP, Henry SC, Hamilton JD, et al. Dendritic cell responses to early murine cytomegalovirus infection: subset functional specialization and differential regulation by interferon alpha/beta. J Exp Med 2003;197:885–898. [PubMed: 12682109]
16. Jinushi M, Takehara T, Tatsumi T, Kanto T, Groh V, Spies T, et al. Autocrine/paracrine IL-15 that is required for type I IFN-mediated dendritic cell expression of MHC class I-related chain A and B is impaired in hepatitis C virus infection. J Immunol 2003;171:5423–5429. [PubMed: 14607946]

17. Asano MTM, Sakaguchi N, Sakaguchi S. Autoimmune disease as a consequence of developmental abnormality of a T cell subpopulation. J Exp Med 1996;184:387–396. [PubMed: 8760792]

18. Nair S, Caspi RR, Nelson LM. Susceptibility to murine experimental autoimmune oophoritis is associated with genes outside the major histocompatibility complex (MHC). Am J Reprod Immunol 1996;36:107–110. [PubMed: 8862255]

19. Zheng Y, Manzotti CN, Burke F, Dussably L, Qureshi O, Walker LS, et al. Acquisition of suppressive function by activated human CD4+ CD25− T cells is associated with the expression of CTLA-4 not FoxP3. J Immunol 2008;181:1683–1691. [PubMed: 18641304]

20. Kim KD, Zhao J, Auh S, Yang X, Du P, Tang H, Fu YX. Adaptive immune cells temper initial innate responses. Nat Med 2007;13:1248–1252. [PubMed: 17891146]

21. Zhao J, Kim KD, Yang X, Auh S, Fu YX, Tang H. Hyper innate responses in neonates lead to increased morbidity and mortality after infection. Proc Natl Acad Sci U S A 2008;105:7528–7533. [PubMed: 18490660]

22. Onishi Y, Fehervari Z, Yamaguchi T, Sakaguchi S. Foxp3+ natural regulatory T cells preferentially form aggregates on dendritic cells in vitro and actively inhibit their maturation. Proc Natl Acad Sci U S A 2008;105:10113–10118. [PubMed: 18635688]

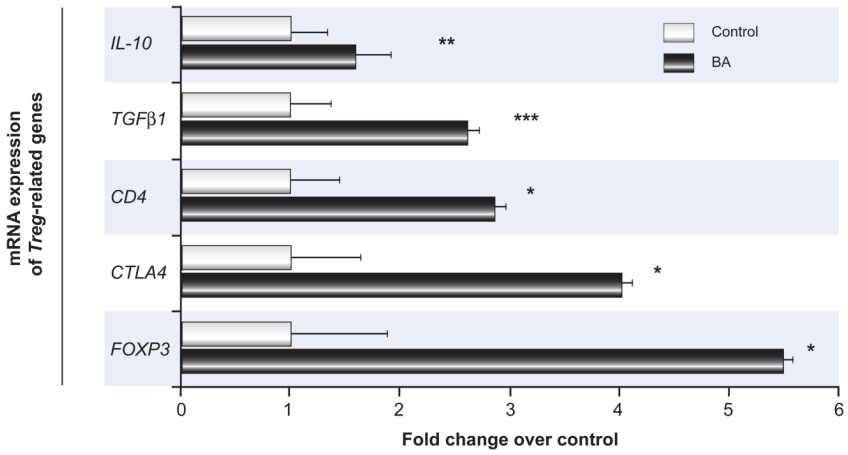

Figure 1. Hepatic expression of Treg-associated genes in children with biliary atresia

Concentrations of hepatic mRNA for candidate genes encoding the Treg cytokines *IL-10* and *TGFβ1*, receptors *CD4* and *CTLA4*, and transcription factor *FOXP3* (vertical axis) were quantified by real-time PCR and expressed as fold change (horizontal axis) in children with biliary atresia (BA) over controls. N=9 for biliary atresia and N=7 for controls; all fold changes are statistically significant with *$p<0.05$, **$p<0.01$, ***$p<0.001$.

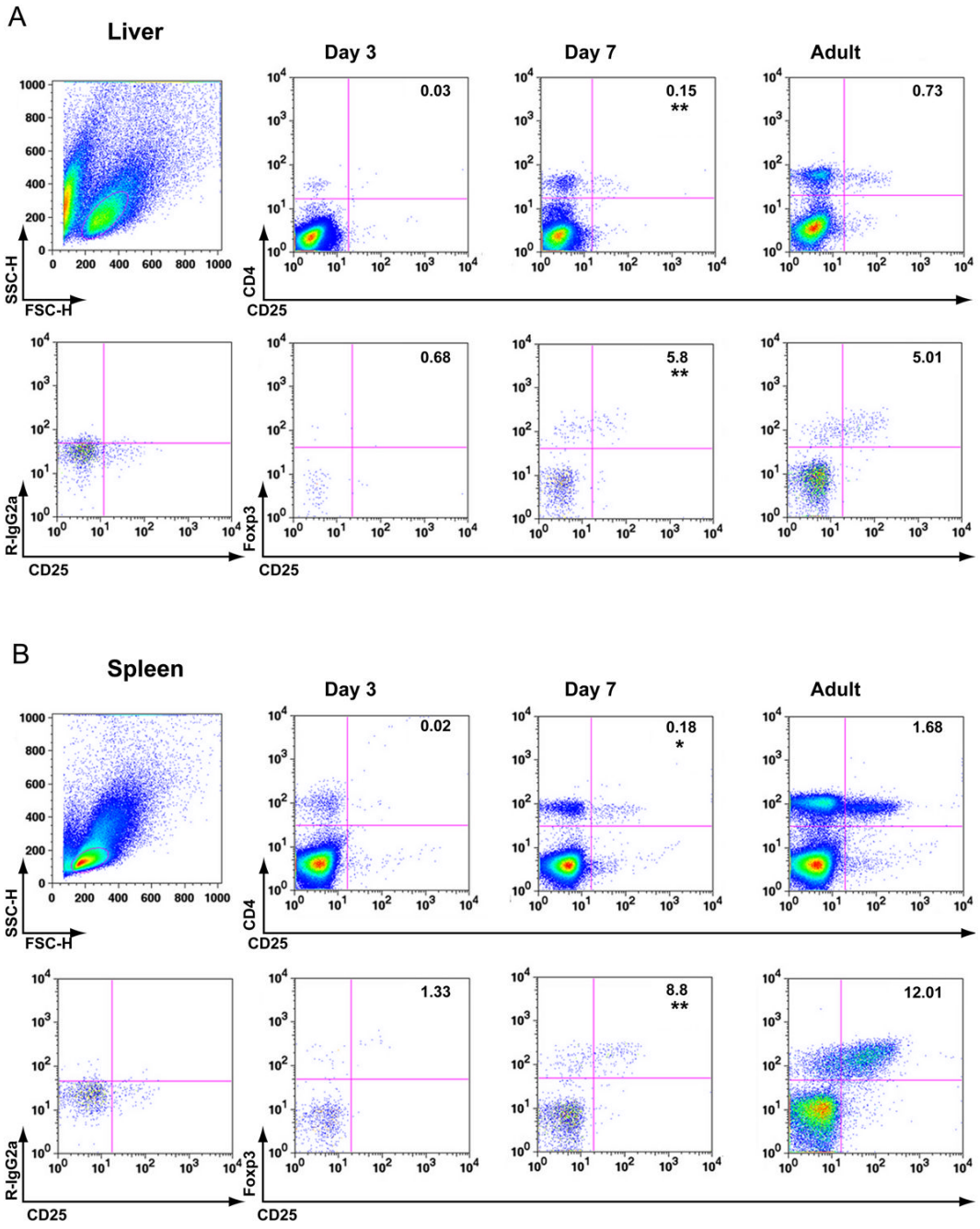

Figure 2. Population of liver and lymphoid tissue with Tregs during ontogeny of BALB/c mice

Flow cytometric quantification of Foxp3+ CD4+ CD25+ Tregs in MNCs from the liver **(A)** and spleen **(B)** of neonatal (3- and 7-day-old) and adult (3-month-old) mice. In both panels, *Top row*: boxed dot plots depict size-gated total lymphocytes (*left column*) stained for the Treg surface markers CD4 and CD25. *Bottom row*: Dot plots depict CD4+ lymphocytes expressing CD25 and the Treg transcription factor Foxp3. Stains with isotype control antibodies were used as negative controls (*left column*). Numbers in both panels represent the average percentage of gated total lymphocytes (top row) or of gated total CD4+ cells (bottom row). Statistical differences between means for groups of 3- and 7-day-old mice are marked with ** ($p \leq 0.005$), * ($p \leq 0.01$), N=3 mice per group and time point.

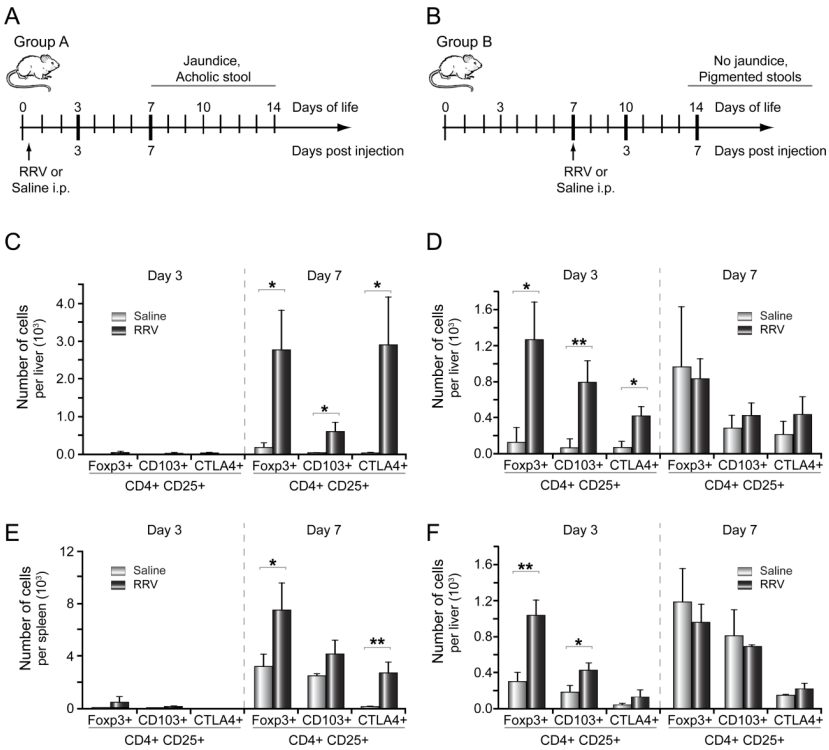

Figure 3. Treg response in liver and lymphoid tissue following RRV infection at birth or on day 7

Panel **A** and **B** display the experimental designs to assess the hepatic Treg responses following RRV infection at the two different time points. Hepatic and splenic subpopulations of Tregs are enumerated by 3-color flow cytometry 3 and 7 days after RRV (or saline control) injection in group A (**C/E**) or group B (**D/F**). The vertical axes display the average number of CD4+ CD25+ cells per organ expressing Foxp3, CD103 or CTLA4 (+S.D.); N=3 for each group and time point with *p<0.05, **p<0.01, RRV *versus* saline (control) group.

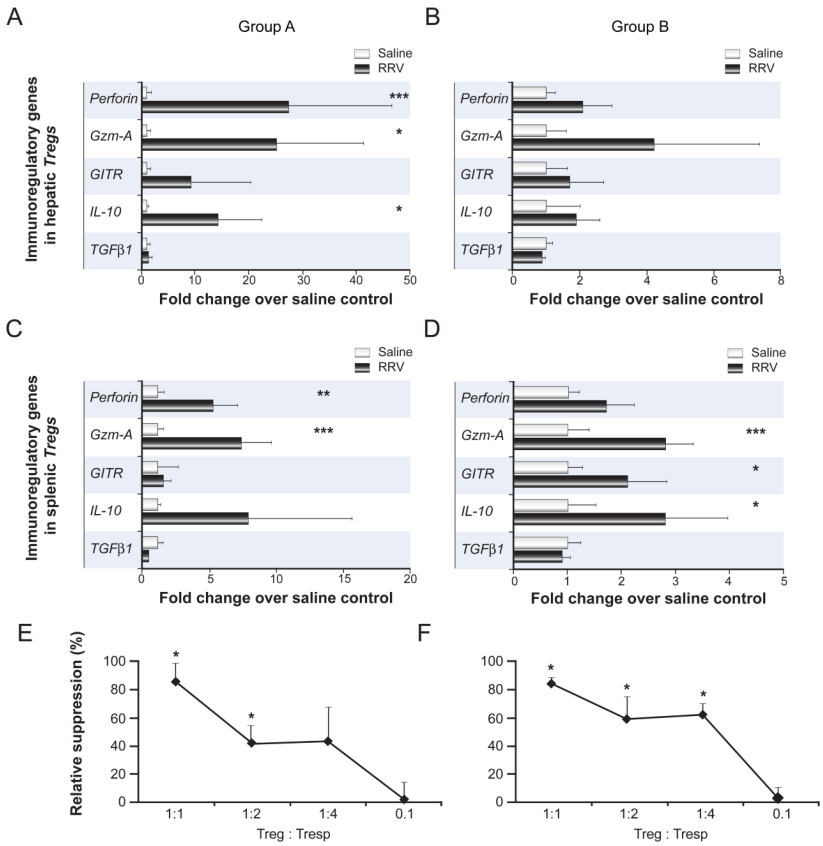

Figure 4. Molecular phenotype and suppressor function of neonatal Tregs emerging after RRV challenge

Panels **A–D** show mRNA expression of activation markers in hepatic (**A/B**) and splenic Tregs (**C/D**) that were purified at the time of Treg emergence following viral challenge in each experimental group, 7 days after RRV injection in group A or 3 days after injection in group B. mRNA levels were quantified by real-time PCR and expressed as average fold change (+S.D.) in Tregs from RRV-infected compared to saline-injected, age-matched controls. N=3–4 independent experiments per group per time point with 6–8 pooled livers/spleens per experiment, *p<0.05, **p<0.01, ***p<0.005, RRV- *versus* control group, Gzm-A; Granzyme-A. Panels **E** and **F** display inhibition of anti-CD3 stimulated proliferation of responder T cells (Tresp) from RRV-infected pups by autologous neonatal Tregs. Neonatal CD25+ Treg and CD25− Tresp CD4+ cells were purified from spleens 7 days after RRV injection into 1-day-old **(E)** or 3 days after injection into 7-day-old pups **(F)**. Maximum proliferation of responder CD4+ in the absence of Tregs was 8300 cpm (mean). The vertical axes display average relative suppression (in %, +S.D.) with * p<0.05, proliferation in presence *versus* proliferation in the absence of Tregs. Percentage of relative suppression was calculated using the formula: 1−(cpm in the presence of Tregs/cpm in the absence of Tregs) ×100. Co-culture assays were performed in triplicate, and results are representative of 2 independent experiments with similar results (8–10 pooled spleens per experiment).

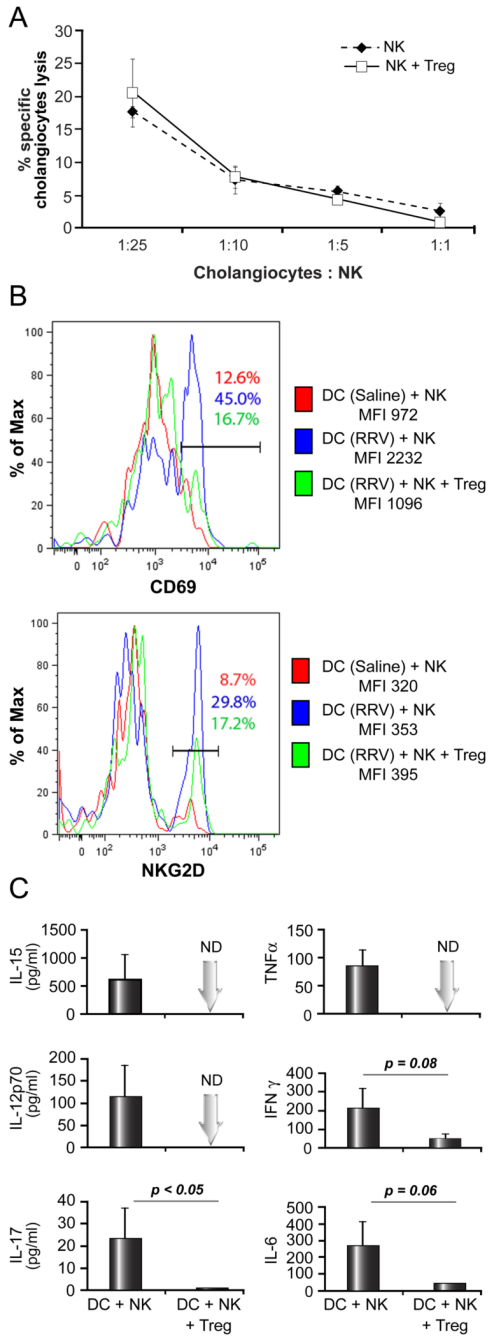

Fig. 5. Modulation of cytolytic function and DC-dependent activation of hepatic NK cells by Tregs in experimental BA

Because of the paucity of Tregs during the first week of life and at the time of initiation of bile duct injury, splenic Tregs from uninfected adult mice were used in these functional assays. In panel **A,** hepatic NK cells are purified 5 days after RRV infection at birth and co-cultured with ^{51}Cr-labeled mCL cholangiocytes for 5 hours. Ratios represent mCL (target) to NK (effector) cells. Tregs were added to the co-culture in a 1:1 ratio with NK cells where indicated. N=3 wells per group; with hepatic NK cells obtained from pools of 10–15 livers. The histograms in panel **B** show representative results of *ex vivo* DC-dependent activation of NK cells as determined by flow-cytometric analysis of NK cell expression of the activation markers

CD69 and NKG2D. Hepatic DC were purified 3 days after RRV inoculation at birth (blue/green) and co-cultured with NK cells purified from livers of non-infected age-matched pups in the presence or absence of Tregs. In control experiments, DC and NK cell populations were both obtained from livers of non-infected 3-day-old pups (red). Panel **C** displays cytokine concentrations measured in supernatants after 24 hours of co-culture of DC+NK or DC+NK +Tregs. Assays were run in duplicate, and the vertical axes display average cytokine levels (+S.D.). ND, not detected; cytokine levels below assay detection limit, MFI, mean fluorescent intensity. DC and NK cells were pooled from 8–12 livers.

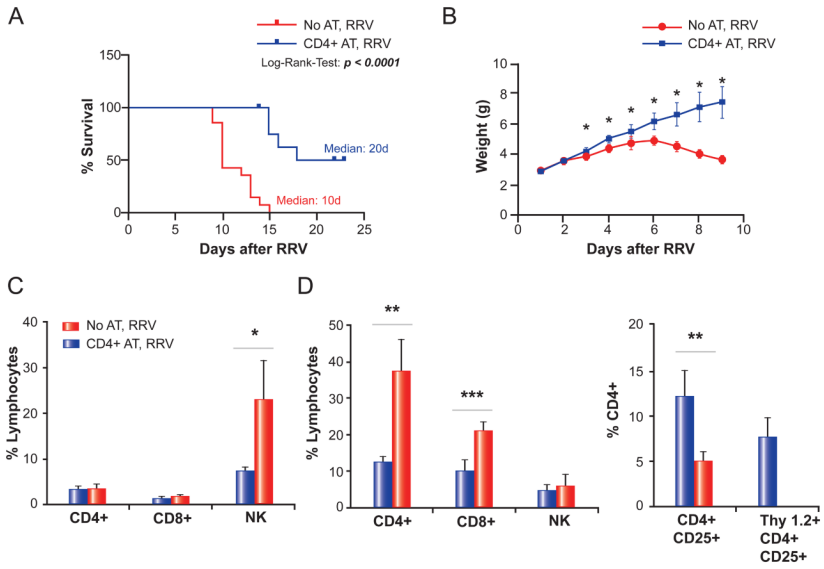

Fig. 6. Effect of adoptive transfer of CD4+ cells on BA-phenotype and hepatic lymphocyte composition

A total of 10×10^6 CD4+ cells were injected i.p. into neonatal Thy1.1+ BALB/c pups on day 2 of life, prior to RRV inoculation the following day (CD4+ adoptive transfer [AT], RRV). Control mice were injected with saline on day 2, prior to RRV inoculation on day 3 (No AT, RRV). Panel **A** displays survival of both groups, plotted according to the method by Kaplan and Meier. N = 13 for CD4+ AT, RRV, and N = 14 for No AT, RRV. Panel **B** shows the daily weights of both groups; N = 8 for each group. In panel **C**, hepatic MNCs were purified 5 days after RRV infection and subjected to flow-cytometric analysis. N=3 for each group. In panel **D**, hepatic lymphocyte composition was analysed by flow cytometry 13 days after RRV infection; N=5 for No AT, RRV, and N = 4 for CD4+ AT, RRV. The vertical axes in panel C and D represent the frequency of size-gated hepatic lymphocytes staining positive for the respective surface markers as percentages. $*p<0.05$, $**p\leq0.01$, $***p\leq0.001$.